

ENERGY SPECTRA BETWEEN 10 AND SEVERAL HUNDRED GeV/NUCLEON FOR
ELEMENTS FROM $_{18}\text{Ar}$ TO $_{23}\text{V}$: RESULTS FROM HEAO-3

V. Vylet^a, C. J. Waddington^b, W. R. Binns^a, T. L. Garrard^c, M. H. Israel^a,
J. Klarmann^a, M. Metzger^a

^a Department of Physics and McDonnell Center for the Space Sciences, Washington University,
St. Louis, MO 63130, USA

^b School of Physics and Astronomy, University of Minnesota, Minneapolis, MN 55455, USA

^c 220-47 Downs Laboratory, California Institute of Technology, Pasadena, CA 91125, USA

ABSTRACT

We report updates of recently published results on cosmic ray energy spectra of the sub-iron nuclei. This paper is based on the following analysis and improvements : a) a better analysis of the charge resolution of the instrument, b) availability of more recent charge-changing cross sections necessary to correct the abundances for interactions inside the detector, and c) a recent revision of the results from the French-Danish C2 experiment on HEAO-3 that were included in our analysis.

INTRODUCTION Data from the Heavy-Nuclei Experiment (HNE) on HEAO-3 were used to determine abundances of the individual elements $_{18}\text{Ar}$, $_{19}\text{K}$, $_{20}\text{Ca}$, $_{21}\text{Sc}$, $_{22}\text{Ti}$ and $_{23}\text{V}$ relative to $_{26}\text{Fe}$ as a function of energy from 10 to several hundred GeV per nucleon. K, Sc, Ti and V are secondary nuclei, i.e. they are mostly fragmentation products of primary nuclei, while Ar and Ca are mixtures of both primary and secondary components. Combining our data with those from the French-Danish experiment (Engelmann *et al.* 1983) on the same spacecraft, which covered the energy range from 1 to 25 GeV per nucleon, the abundances of the secondary elements relative to Fe were fitted by power laws in energy, aE^p . Ar and Ca abundance ratios to Fe were fitted by $aE^p + b$ where b is the primary component.

INSTRUMENTATION AND DATA ANALYSIS The HNE detector consisted of a stack of six dual gap ionization chambers, divided into 2 modules. Each module had an x-y multiwire ionization hodoscope on its top and bottom. In the center of the stack was placed a Cherenkov counter consisting of radiators mounted on both sides of a light diffusion box.

In the event selection, a geomagnetic cutoff rigidity of at least 8 GV was required. The energy of the particles was determined using the "relativistic rise", i.e. the logarithmic increase of charged particle energy loss with increasing energy over the interval from a few GeV to several hundred GeV per nucleon. The ionization chamber signal I can be described as

$$I = Z^2 f(\beta)$$

where $f(\beta)$ is normalized to unity at its minimum near $\beta = 0.96$ (2.6 GeV per nucleon) and rises approximately as the logarithm of the energy at higher energies. Ionization signals are normalized so that $Z_1 = \sqrt{I} \approx Z$ for a minimum ionizing nucleus. Since for the energies considered here ($\beta \geq 0.97$) the Cherenkov signal C is proportional to Z^2 , we can define $Z_c = \sqrt{C}$ in charge units so that it is, after an appropriate normalization, very close to the charge Z of the particle. The energy was determined from the relativistic rise ρ defined as

$$\rho = \frac{Z_1}{Z}$$

Several selection criteria, based on the consistency of signals within and between the two groups of ionization chambers as well as the photomultipliers on the Cherenkov light box, eliminated events with large charge-changing interactions within the detector, coincident extraneous particles, accidental hits of one photomultiplier, etc. Those small charge-changing reactions that could not be filtered out using the selection criteria were corrected by calculation based on measured cross sections.

To translate the abundances relative to Fe to the energy scale, a p -to-mean-energy conversion function was determined by an iterative procedure described in detail in our previous work (Binns *et al.* 1988). The conversion function is dependent on the slope, p , of the energy spectrum and the charge resolution, σ_{z_1} , of the instrument, these values being used in the "smearing" procedure that calculates the conversion function. To find the slopes, p , of the relative abundances to Fe of the secondary elements, our data (Binns *et al.* 1988) are combined with those from the French-Danish experiment and fitted with aE^p . New relative abundances are calculated and the whole cycle is repeated until a stable value of p is achieved. Slope values for Ar and Ca are obtained by interpolation using a weighted fit to the p values for the secondary elements as illustrated in figure 1. Their relative abundances are fitted by $aE^p + b$. Similarly to the secondary elements, several iterations are performed, this time keeping p constant with a and b being free parameters. This type of fit is a simple way to separate the primary and secondary components. A more elaborate approach can be found in the paper presented by Mewaldt and Webber at this conference (OG 8.3-17).

NEW RESULTS Originally, in the procedure used to correct for the interactions in the honeycomb lid and the detector, the partial charge-changing cross sections for Fe on Al were not available; those for Fe on C were used instead. Thanks to availability of recent data for Fe on Al (Cummings 1989) we recalculated the abundances at the top of the detector. This correction changed the previously obtained results only very slightly.

Although we reported that our previous fitting procedure assumed that σ_{z_1} was independent of Z and equal to 0.4 cu, in fact those fits assumed that σ_{z_1} was proportional to Z . Further analysis has refined this linear dependence on Z , with σ_{z_1} varying from 0.277 cu for Ar to 0.421 cu for Fe. These improved estimates of σ_{z_1} lead to changes of the slopes of the relative abundance spectra by no more than one standard deviation.

The original data from the French-Danish experiment covered the energy range from 1 to 25 GeV per nucleon and were in good agreement with our data in the overlap region. The recently extended abundances (Engelmann *et al.* 1989) span the range from 0.8 to 35 GeV per nucleon. As can be seen from figure 2, the agreement with our data over the wider overlap interval is maintained and even shows a slight improvement for V, Ar and Ca. From the comparison in table 1 of the new and previous slopes of the relative abundances versus energy, a systematic shift of approximately one standard deviation is apparent. The primary components of the Ar and Ca relative abundances also changed only very slightly: from 0.026 ± 0.007 to 0.024 ± 0.005 for Ar and from 0.088 ± 0.007 to 0.086 ± 0.006 for Ca. The above results are based on the assumption that p has a dependence on Z as illustrated in figure 1. Further tests showed that even under the extreme assumption of a constant $p = -0.28$ for all elements considered here, the primary component remains almost unchanged for Ca and is reduced by less than a factor of 2 for Ar. Numerical values of the abundances relative to Fe derived from our experiment are presented in table 2.

CONCLUSIONS We have updated our previously published energy spectra of cosmic rays for elements with $Z=18$ to 26 using the new data from the French-Danish experiment, better partial charge-changing cross sections and improved evaluation of the charge resolution in our instrument. The latter modification is the most responsible for changes in the slopes of the energy spectra for secondary elements and the change of the primary component for Ar and Ca. However, these changes remain within one standard deviation and do not alter our previous conclusions: a) the energy spectra of the sub-iron secondary elements relative to Fe exhibit a power-law decrease up to ~ 150 GeV, b) Ar and Ca have substantial secondary components at low energies that decrease with increasing energy, and c) the primary abundances of Ar and Ca relative to Fe agree with values inferred from lower energy data and confirm a fractionation of source abundances in which elements with high values of the first ionization potential are depleted relative to those with low first ionization potential.

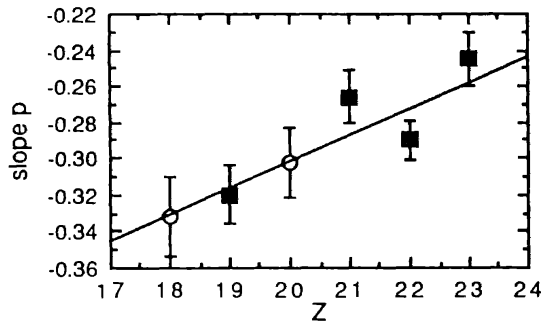


Figure 1 : Slopes of Ar and Ca spectra (open circles) are obtained by interpolation from the fit to the secondaries (solid squares).

Z	p exponent	
	current value	Binns et al 1988
[18]	-0.332 ± 0.021	-0.321 ± 0.028
19	-0.320 ± 0.016	-0.310 ± 0.010
[20]	-0.302 ± 0.019	-0.291 ± 0.010
21	-0.266 ± 0.015	-0.250 ± 0.020
22	-0.290 ± 0.011	-0.280 ± 0.010
23	-0.245 ± 0.015	-0.230 ± 0.020

Table 1 : Comparison of the current slopes of the energy spectra relative to Fe with previously published values. The values for Ar and Ca are estimated slopes of their secondary components inferred from figure 1.

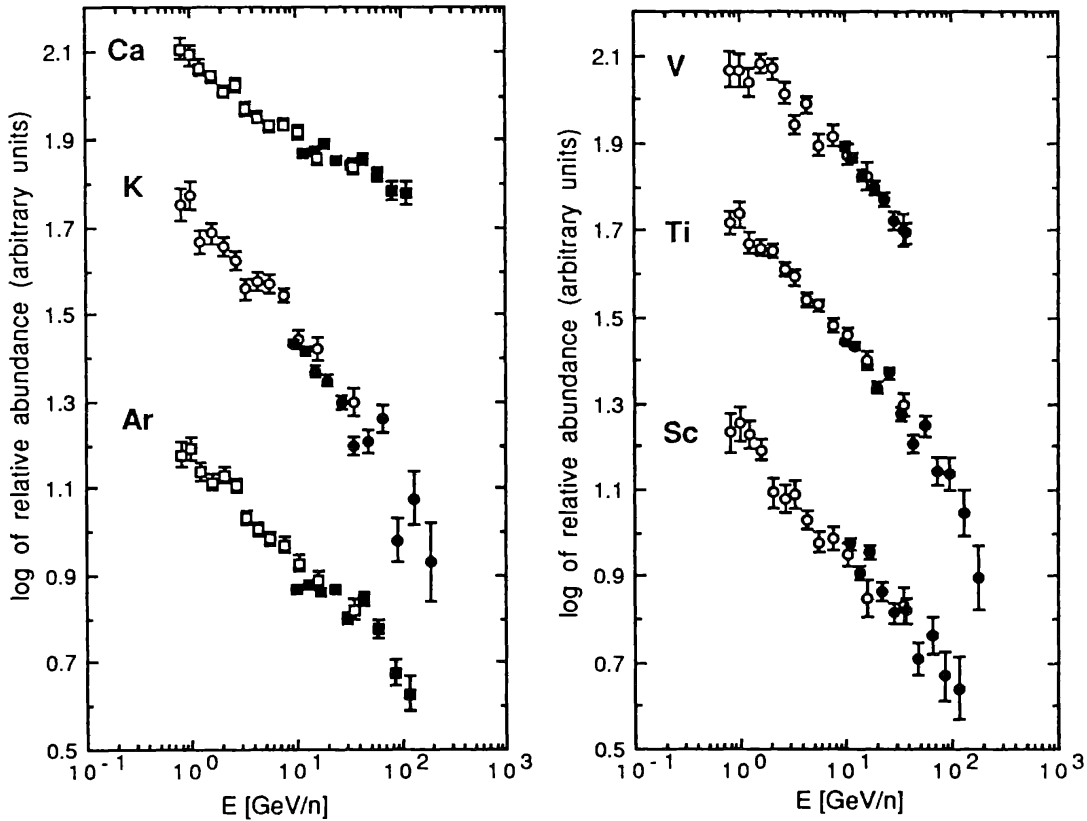


Figure 2 : Plot of abundances relative to Fe in arbitrary units. Open symbols denote data from the French-Danish experiment while filled points are our data. Circles are used for the secondary elements and squares for Argon and Calcium. Numerical data are presented in table 2.

K	E [GeV/n]	rel. abd.	st. dev.
	9.55	0.0542	0.0011
	12.04	0.0522	0.0012
	15.40	0.0468	0.0013
	19.96	0.0445	0.0015
	26.44	0.0398	0.0016
	35.72	0.0316	0.0016
	48.53	0.0323	0.0021
	65.97	0.0365	0.0027
	90.60	0.0191	0.0023
	127.42	0.0238	0.0036
	184.19	0.0170	0.0040

Ti	E [GeV/n]	rel. abd.	st. dev.
	10.22	0.0879	0.0015
	12.62	0.0861	0.0017
	15.70	0.0777	0.0018
	19.71	0.0689	0.0019
	25.15	0.0747	0.0022
	32.47	0.0602	0.0023
	42.44	0.0512	0.0024
	55.48	0.0560	0.0030
	72.54	0.0439	0.0032
	96.02	0.0433	0.0039
	129.68	0.0352	0.0047
	178.84	0.0250	0.0048

Sc	E [GeV/n]	rel. abd.	st. dev.
	10.82	0.0299	0.0009
	13.48	0.0257	0.0009
	17.00	0.0286	0.0011
	21.66	0.0231	0.0011
	28.15	0.0206	0.0012
	37.03	0.0209	0.0014
	49.12	0.0162	0.0015
	64.98	0.0183	0.0019
	86.65	0.0148	0.0021
	117.68	0.0138	0.0025

V	E [GeV/n]	rel. abd.	st. dev.
	9.81	0.0495	0.0012
	11.98	0.0465	0.0013
	14.74	0.0422	0.0014
	18.29	0.0398	0.0015
	22.97	0.0372	0.0016
	29.22	0.0334	0.0017
	37.59	0.0312	0.0018

Ar	E [GeV/n]	rel. abd.	st. dev.
	9.99	0.0739	0.0011
	12.92	0.0760	0.0014
	16.92	0.0730	0.0017
	22.60	0.0739	0.0020
	30.79	0.0635	0.0021
	42.83	0.0700	0.0027
	59.67	0.0599	0.0030
	83.43	0.0477	0.0034
	119.30	0.0426	0.0042

Ca	E [GeV/n]	rel. abd.	st. dev.
	11.79	0.1474	0.0018
	14.88	0.1496	0.0021
	19.01	0.1555	0.0025
	24.73	0.1419	0.0028
	32.85	0.1394	0.0033
	44.29	0.1430	0.0040
	59.85	0.1320	0.0047
	81.10	0.1213	0.0055
	111.82	0.1199	0.0072

Table 2 : Abundances of the sub-iron elements relative to Fe and their standard deviations as a function of energy per nucleon.

ACKNOWLEDGEMENTS This research was supported in part by NASA grants NAG8-498, 500, 502 and NGR 05-002-160, 24-005-050 and 26-008-001. The assistance of E. C. Stone is gratefully acknowledged.

References

- Binns, W. R., Garrard, T. L., Israel, M. H., Jones, M. D., Kamionkovski, M. P., Klarmann, J., Stone, E. C. and Waddington, C. J., *Ap. J.*, 324, 1106, 1988.
 Cummings, J. R. 1989, PhD Thesis, University of Minnesota, Minneapolis.
 Engelmann, J.-J., *et al.* 1983, *Proc. 18th Int. Cosmic Ray Conf.* (Bangalore) 2, 17.
 Engelmann, J.-J., Ferrando, P., Goret, P., Koch-Miramond, L., Masse, P., Petrou, N., Soutoul, A., Juliusson, E., Lund, N., Peters, B., Rassmussen, I. L. , - submitted to *Astronomy and Astrophysics* ,1989.